Ambiphilic Reactivity of SF5-Alkynes Applied to Regioselective and Stereodivergent Halogenation Reactions: An Experimental and Theoretical Case Study

David Matchavariani, Lucas Popek, Jorge Juan Cabrera-trujillo, Thi Mo Nguyen, Nicolas Blanchard, Karinne Miqueu, Dominique Cahard, Vincent Bizet

RESEARCH ARTICLE doi.org/10.1002/adsc.202400446

Ambiphilic Reactivity of SF_5-Alkynes Applied to Regioselective and Stereodivergent Halogenation Reactions: An Experimental and Theoretical Case Study

David Matchavariani,[a] Lucas Popek,[a] Jorge Juan Cabrera-Trujillo,[c] Thi Mo Nguyen,[b] Nicolas Blanchard,[a] Karinne Miqueu,[c,*] Dominique Cahard,[b,*] and Vincent Bizet[a,*]

[a] Université de Haute-Alsace, Université de Strasbourg, CNRS, LIMA, UMR 7042, 68000 Mulhouse, France
E-mail: vbizet@unistra.fr
[b] CNRS, UMR 6014 COBRA, Normandie Université, 76821 Mont Saint Aignan, France
E-mail: dominique.cahard@univ-rouen.fr
[c] CNRS/Université de Pau et des Pays de l'Adour, E2S-UPPA, IPREM UMR 5254, 64053 Pau cedex 09, France
E-mail: karinne.miqueu@univ-pau.fr

Manuscript received: April 18, 2024; Version of record online: ■■, ■■

Supporting information for this article is available on the WWW under https://doi.org/10.1002/adsc.202400446

Abstract: We explored the ambiphilic reactivity of SF_5-alkynes, and we proved they can act as both nucleophiles and electrophiles. We selected halogenation reactions as benchmark reactions and developed highly selective stereodivergent hydrohalogenation (I, Br, Cl, F) reactions of SF_5-alkynes. The stereochemistry is finely controlled thanks to the nature of the acids used (strong or soft) in the presence of halide source, while the high regioselectivity is governed by the strong polarization of SF_5-alkynes. Mechanistic studies supported by DFT calculations shed light on two different reaction mechanisms responsible of the excellent stereocontrol. This stereoselectivity was quantitatively rationalized with the ASM and EDA methods. A few dihalogenation reactions are reported and DFT calculations rationalize this *cis*-stereoselectivity. Relative configuration of all the SF_5-haloalkenes was unambiguously determined by X-ray diffraction. Noteworthy, several post-functionalization reactions such as cross-couplings, cyanation and reductions are described to strengthen the synthetic potential.

Keywords: pentafluorosulfanyl; halogenation; SF_5-alkyne; regioselective and stereodivergent; DFT

Introduction

Nowadays, the pentafluorosulfanyl group (SF_5)[1] is on the way to become an essential fluorinated group in many fields such as heterocyclic synthesis,[2] medicinal chemistry,[3] drug development,[4] and materials science.[5] The current craze for this motif is so far limited by the few strategies available to reach sufficient molecular diversity, which rely either on direct radical pentafluorosulfanylation of aliphatic unsaturated compounds,[6] or on oxidative fluorination of sulfur derivatives.[7] SF_5-Alkynes[8] and R-SF_4-alkynes[9] are versatile substrates that have yet to reveal their full synthetic potential. Recently, we developed a fully regio- and stereoselective hydroelementation of SF_5-alkynes with N-, O- and S-nucleophiles, where the SF_5-alkynes were acting as good electrophiles.[10] Indeed, the strong polarization of SF_5-alkynes towards the SF_5 group was calculated to have a charge difference $\Delta q = 0.39$ with $qC_\alpha = -0.298$ and $qC_\beta = +0.090$ (with R = *p*-Ph-C_6H_4), which makes the C_β electrophilic and the C_α nucleophilic. To pursue our efforts to develop highly regio- and stereoselective transformations we wondered if polarized SF_5-alkynes could react in an ambiphilic manner either as electrophiles or nucleophiles. Thus, we selected the hydrohalogenation

reaction of SF_5-alkynes as benchmark transformation.[11] Thanks to charge difference, we expected high regioselectivity for the halogenation while the stereoselectivity could be modulated by reaction mechanism. Indeed, only a few examples of SF_5-haloalkenes are known in the literature, most of them resulting from the radical introduction of SF_5Cl or SF_5Br onto alkynes (Scheme 1a–c).[12] A single example of *β,Z*-fluoro SF_5-olefin was reported by Paquin in 2019 by gold-catalyzed hydrofluorination but in only 15% yield (Scheme 1d).[13] In 2023, we proposed the synthesis of *β,E*-iodo SF_5-olefins *via* the direct iodopentafluorosulfanylation of alkynes, but SF_5-iodoolefins are in some cases obtained in a mixture with SF_5-chloroolefins (Scheme 1e).[14] In the present study, we made the assumption that SF_5-alkynes could act as electrophiles in reaction with nucleophilic halides, and as nucleophiles in reactions with electrophilic species such as strong acids or dihalogens. We anticipated that the nature of the halide and the mechanism involved should have a strong impact on the regio- and stereoselectivity. The aim of this fundamental study is to illustrate the ambiphilic reactivity of SF_5-alkynes and to gain a better understanding *via* DFT mechanistic studies.

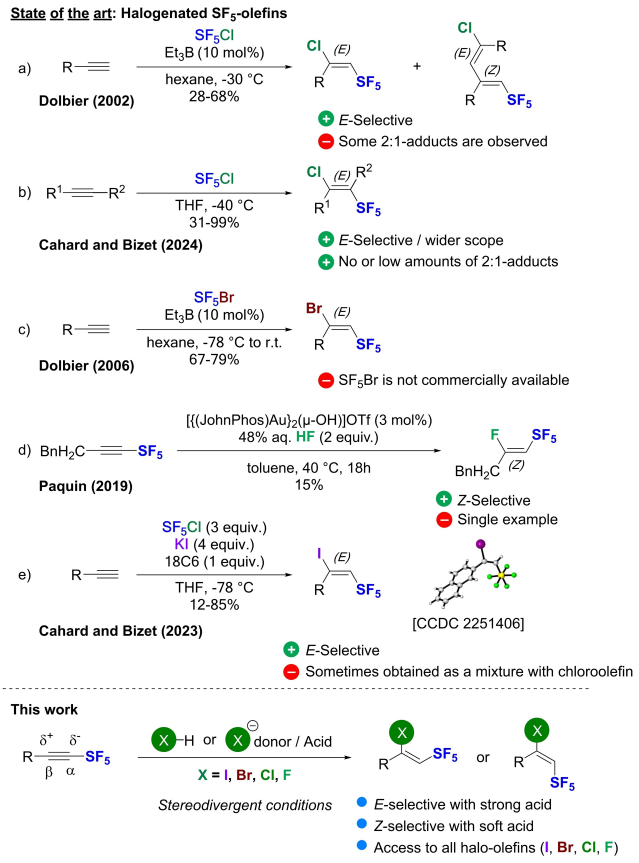

Scheme 1. State of the art access to SF_5-halo-olefins and proposed strategy for the hydrohalogenation of SF_5-alkynes.

Results and Discussion

At the outset, we considered that SF_5-alkynes could act as nucleophiles. We started our investigation with the hydroiodination of SF_5-alkyne **1a** using an aqueous solution of hydroiodic acid (57%)[15] in toluene at 80 °C and we were delighted to observe full conversion of the SF_5-alkyne into a single regio- and stereoisomer **2a** isolated in 85% yield (Conditions A, Scheme 2). The scope and limitations of the substrates were investigated to demonstrate a unique stereoselectivity and good to high yields were obtained with various aromatic (**2a–o**) and heteroaromatic alkynes (**2p–q**). The configuration was unambiguously determined by single-crystal X-ray diffraction (SCXRD) analysis of **2k** [CCDC 2251406][16] to be the *β,E*-isomer and we assumed that all other products have the same *E* configuration as they share the same NMR spectral characteristics. The *p*-NO_2 phenyl SF_5-alkyne **1h**, which is strongly deactivated proved to be poorly reactive with HI leading at best to 39% NMR yield of **2h** along with 8% of **3h** and 13% of **4h** after 20 h reaction with 5 equiv. of HI. Interestingly, with alternative conditions using nBu_4NI and TFA, increasing the quantity of nBu_4NI from 1.5 to 5 equivalents helped to improve the conversion up to 90%, but **3h** became the major product (52% NMR yield) along with 21% of **2h** and 17% of **4h**. This poorly nucleophilic alkyne **1h** is a particular case that seems

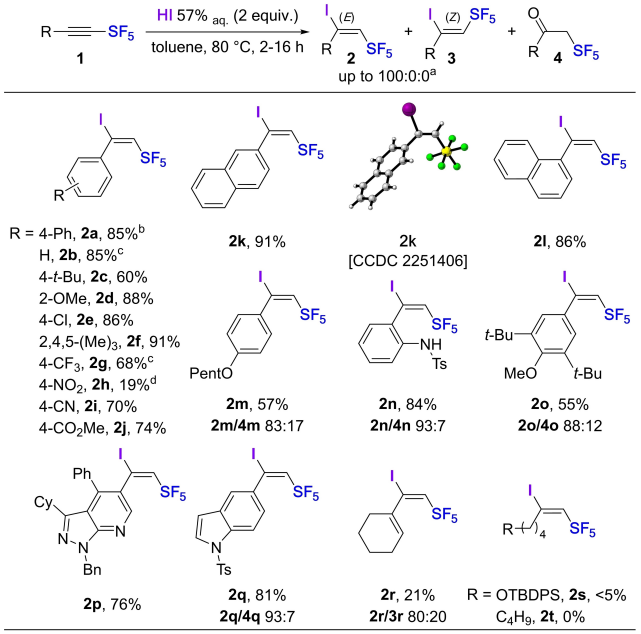

Scheme 2. Conditions A: Hydroiodination of SF_5-alkynes with aqueous HI solution.[a] Unless otherwise noted, **2** was formed as single product. [b] Performed with 1.5 equiv. of HI (57% aq.). [c] Performed with 3 equiv. of HI (57% aq.). [d] Performed with 5 equiv. of HI (57% aq.).

to favor the mechanism of conditions B (*vide infra*). For few substrates **1m–o** and **1q**, a small amounts of ketones **4** were observed due to partial hydrolysis. Vinylogous alkyne **1r** was the only example where we observed a small fraction of *β*,*Z*-isomer **3r**, while alkyl substituted substrates **1s–t** were unreactive under these conditions.

Next, we evaluated SF_5-alkynes as electrophiles with halide salts. For this purpose, we used a combination of sodium iodide in acetic acid at 110 °C[11] and we were pleased to observe full conversion of SF_5-alkyne **1a** with the formation of the *β*,*Z*-isomer **3a** as single product, isolated in 91% yield (Conditions B, Scheme 3) with stereochemistry confirmed by SCXRD analysis [CCDC 2303461]. The scope of this reaction is much more general than for conditions A as it tolerates aromatic (**3a–o**), heteroaromatic (**3q**), vinyl (**3r**) and even alkyl (**3s–t**) substituents, affording good to high yields. A limitation was observed with alkynes **1i** and **1j**, substituted by a cyano and an ester function, respectively, for which reduced *E*-products **5i–j** were observed for the first time. (*Z*)-Pentafluoro(2-iodovinyl)-λ^6-sulfane **3u*** was obtained as a single product starting from silylated alkyne **1u** (R = $SiEt_3$). We assume that the expected vinylsilane **3u** was formed over the course of the reaction and rapidly underwent desilylation. These results clearly pointed out to an ambivalent reactivity of SF_5-alkynes; next, we wondered what would be the reactivity of these substrates in dihalogenation reactions (Conditions C, Scheme 4).[17] Reaction of SF_5-alkyne **1a** with iodine in dichloromethane led to the formation of a 86:14 *Z*/*E* mixture of stereoisomers (**6a**/**7a**). We successfully isolated the *Z*-isomer **6a**, but it appeared to be sensitive and prompt to deiodination over time leading to the partial recovery of **1a** along with the appearance of a pink color.[18] The diiodination was successfully extended to aromatic alkyne **1k** but was not effective with alkyl alkyne **1t**. The reaction with iodine monochloride was also effective yielding a single regioisomer with introduction of the iodine atom in *α*-position of the SF_5 and the chlorine atom in *β*-position exclusively (confirmed by SCXRD analysis [CCDC 2303457]), in a *Z*/*E* ratio >90:10, with products **6a'** and **6k'** isolated in 90 and 86% yields, respectively. Unfortunately, once again the reaction was not effective with alkyl substrate **1t**. Finally, the reaction with bromine was fully stereoselective with aromatic substrates delivering the *Z*-isomers **6a"** and **6k"** in excellent 99 and 90% yields (confirmed by SCXRD analysis of **6k"** [CCDC 2303458]). Moreover, alkyl alkyne **1t** was well tolerated in this case even if a moderate *Z*/*E* ratio of 78:22 (**6t"**/**7t"**) was obtained.

Capitalizing on these results, we wondered if the stereodivergent hydroiodination reactions (Conditions A and B) could be extended to other halogens (Scheme 5a). Replacing HI in conditions A with HBr or HCl, we consistently obtained selectivity for the *E*-isomer. Using HBr, a messy mixture of products was

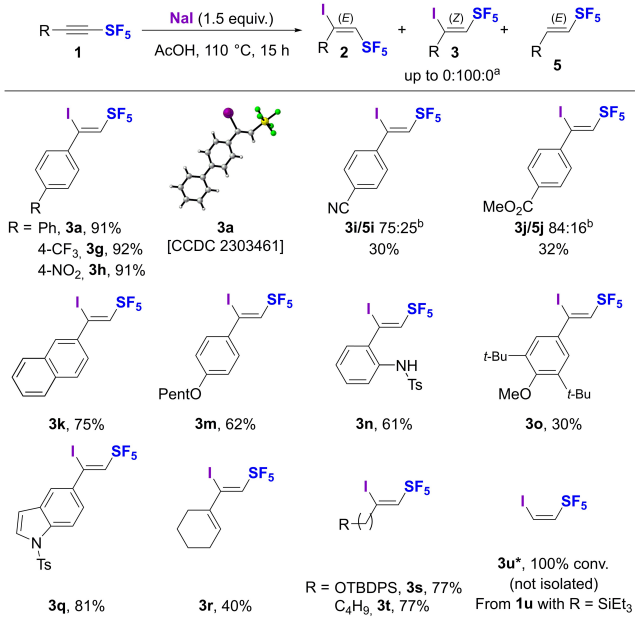

Scheme 3. Conditions B: Hydroiodination of SF_5-alkynes with NaI in AcOH. [a] Unless otherwise noted, **3** was formed as single product. Product **3u*** was obtained from $Et_3Si–C{\equiv}C–SF_5$ **1u**. [b] Similar ratios were obtained either using NaI or Bu_4NI.

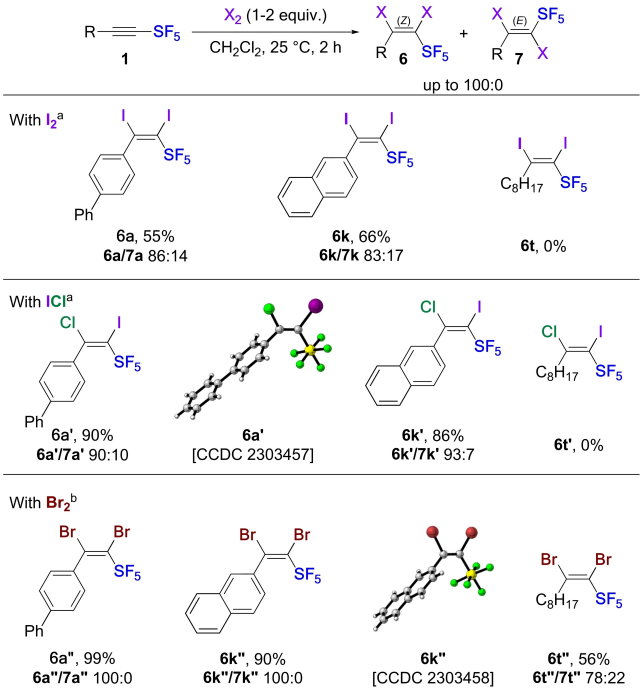

Scheme 4. Conditions C: Dihalogenation of SF_5-alkynes with I_2, ICl and Br_2. [a] Performed with 2.0 equiv. of I_2 or ICl. [b] Performed with 1.0 equiv. of Br_2.

a) Evaluation of halides in conditions A and B (**1a**, R = *p*-Ph-C_6H_4)

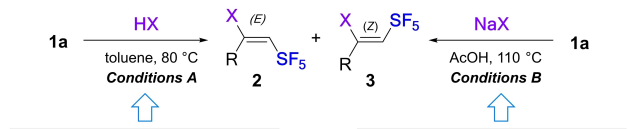

Acid	Conv.(%)	2/3 (%)[a]		2/3 (%)[a]	Conv.(%)	Salt
HI (57% aq.)	100	100:0	2a/3a	0:100	100	NaI
HBr (48% aq.)	62	17:0[b]	2aa/3aa	16:31[b,c]	100	NaBr
HCl (37% aq.)	100	94:0[c]	2ab/3ab	18:50[c]	71	NaCl
HF (40% aq.)	0	-	2ac/3ac	-	0	NaF

b) Revisited conditions A and B by changing acids and halides

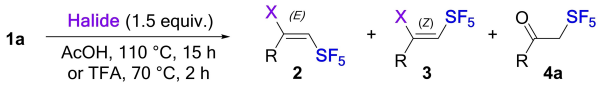

Conditions	Acid	Halide	Conv.(%)	2/3 (%)[a]	
A1	TFA	NaBr	100	29:0[d]	2aa/3aa
A2	TFA	*n*Bu$_4$PBr	100	100:0	2aa/3aa
B2	AcOH	*n*Bu$_4$PBr	100	0:100	2aa/3aa
A3	TFA	Me$_4$NCl	100	85:2[d]	2ab/3ab
B3	AcOH	Me$_4$NCl	100	0:98[c]	2ab/3ab
A4	TFA	*n*Bu$_4$NF	100	0:0[d]	2ac/3ac
B4	AcOH	*n*Bu$_4$NF	13	0:0[c]	2ac/3ac
B4'	-	*n*Bu$_4$NF	100	0:100[e]	2ac/3ac
A4'	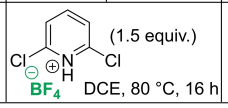 (1.5 equiv.) DCE, 80 °C, 16 h		100	55:6[c]	2ac/3ac

Structures confirmed by SCXRD analysis

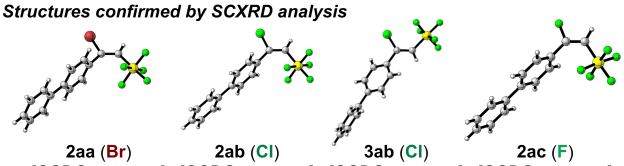

2aa (Br) [CCDC 2303456] **2ab** (Cl) [CCDC 2303459] **3ab** (Cl) [CCDC 2303460] **2ac** (F) [CCDC 2303462]

Scheme 5. Evaluation of acids and halide sources. [a] NMR yields were determined by ^{19}F-NMR using $PhCF_3$ as internal standard. [b] A messy mixture of brominated products was obtained. [c] Small amounts of α-SF_5-ketone **4a** was observed coming from partial hydrolysis of **1a**. [d] Products of addition of TFA were observed by ^{19}F-NMR leading to the formation of α-SF_5-ketone **4a** after workup. [e] Conditions B4': TBAF (1 M in THF, 1.5 equiv.), THF, r.t., 1 h.

observed but no trace of the *Z*-isomer. Unfortunately, no reaction occurred in the presence of aqueous solution of HF. Under conditions B, we first noticed that NaBr, NaCl or NaF were poorly soluble in acetic acid, resulting in poor reactivity and selectivity. Addition of a small amount of water enhanced the solubility of the salt and the homogeneity of the whole mixture was attained at 110 °C. With NaBr, a mixture of *E*/*Z* isomers (**2aa**/**3aa**) was obtained in 16% and 31% NMR yields, respectively, alongside with ketone **4a** and other by-products. With NaCl, the reaction was cleaner affording **2ab**/**3ab** in 18 and 50% ^{19}F-NMR yields, respectively. Even if *E*/*Z* ratios were lower than with NaI, we could notice that the *Z*-isomers were always favoured as major products under conditions C. However, no reaction took place with sodium fluoride. This difference in reactivity and selectivity depending on the nature of the halide raised several fundamental questions, such as the influence of the pKa of the acid, the difference of nucleophilicity of the halides as well as solubility issues. For a better understanding of these reactions, we carried out experiments using strong acids with various halide sources to mimic conditions A, and we tested more soluble halide sources with soft acetic acid for variation of conditions B.

Initially, we focused our effort on hydrobromination reaction (Scheme 5b) and we found that using the combination of trifluoroacetic acid (TFA) and sodium bromide in place of HBr, we were able to get the single stereoisomer **2aa** in up to 29% yield (Conditions A1). More interestingly, using TFA and *n*Bu$_4$PBr (Conditions A2) we reached 100% selectivity for the *E*-isomer **2aa** in quantitative yield. This excellent result encouraged us to compare the bromide sources under soft acidic conditions B. We found that *n*Bu$_4$PBr in acetic acid yielded exclusively the *Z*-isomer **3aa** (Conditions B2) and compared favourably with the use of NaBr probably for solubility reasons. These results indicate that protonation of the alkyne by means of a strong acid is required in conditions A, and a good solubility of the halide source is necessary for the reaction to proceed, especially in conditions B. We then confirmed this finding by extending this reactivity to hydrochlorination. The same trend was observed with the *E*-isomer **2ab** being predominantly obtained in conditions A3 (85% ^{19}F-NMR yield) whereas the *Z*-isomer **3ab** was the unique product in conditions B3 (98% ^{19}F-NMR yield) (Scheme 5b). We also confirmed that conditions B2 and B3 were suitable with the aliphatic substrate **1t**, delivering products **3ta** and **3tb** in 69 and 76% yield, respectively.[19] For reactions performed in TFA in the presence of moderately nucleophilic halides, *i.e.* NaBr and Me$_4$NCl, trace amount addition of TFA on **1a** was observed, but the corresponding enol trifluoroacetate is too sensitive to hydrolysis and delivers the α-SF_5-ketone **4a** after hydrolysis. In attempts to carry out hydrofluorinations, the use of TBAF as a fluoride salt in conditions A4 and B4 was unsuccessful (Scheme 5b). In conditions A4 with TFA, full conversion was observed to form α-SF_5-ketone **4a** as main product coming from the protonation of the alkyne followed by addition of TFA anion or water (observed by NMR) rather than fluoride anion. In conditions B4, only 13% conversion into α-SF_5-ketone **4a** was observed.

After some optimization, we were very pleased to find that by simplifying the conditions B4 to conditions B4' (Scheme 5b) with addition of TBAF solution (1 M

in THF) without acid and by carrying out the reaction at room temperature, we were able to perform fully selective hydrofluorination to get *ß*,*Z* product **3ac** *via* nucleophilic addition of fluoride anion followed by protonation with water contained in TBAF solution. During the writing of the present article, same conditions for *Z*-selective hydrofluorination of SF_5-alkynes and pyridines-SF_4-alkynes have been discovered and reported by the group of Shibata, which highlights the emulation of this research topic.[20] In addition, inspired by the work from Liu and Wang,[21] we successfully obtained the *ß*,*E* isomer (55% of **2ac**) by using an excess of 2,6-dichloropyridinium tetrafluoroborate in DCE at 80 °C. This result is beyond the context of the present study and was not further optimized. Structures of **2aa** [CCDC 2303456], **2ab** [CCDC 2303459], **3ab** [CCDC 2303460] and **2ac** [CCDC 2303462] were unambiguously determined by SCXRD analysis.

In order to have better insights on the mechanisms and on the stereocontrol of the dihalogenation and hydrohalogenation reactions involving SF_5-alkynes, we carried out Density Functional Theory (DFT) calculations at the PCM(solvent)-B3LYP-D3(BJ)/6-311G** level of theory.[19] In the initial phase of our investigation, our focus was directed towards the computational study of dihalogenation reactions (conditions C). To this end, we chose to explore the dibromination reaction as model reaction, as it can occur both in the presence of aromatic or alkyl substituents on the alkyne. Moreover, experimentally it has been shown that the nature of the substituent influences the stereoselectivity outcome. Our experimental results revealed that dibromination reactions of SF_5-alkynes featuring an aromatic substituent led uniquely to *Z*-isomer. On the contrary, with an alkyl substituent a *Z*:*E* ratio of 78:22 was obtained (Scheme 4). The intriguing nature of this phenomenon prompted us to investigate more closely this case and try to rationalize it through DFT calculations. Dibromination reactions of alkynes are generally accepted to proceed *via* the electrophilic addition of a bromonium cation, thereby forming a bridged or open cationic intermediate.[22] Such electrophilic addition has been proposed to be facilitated by a second molecule of Br_2, which favours the breaking of the Br–Br bond.[23] Consequently, we considered two molecules of Br_2 in our computational study. We proposed that a 1:2 π-complex is first formed between the SF_5-alkyne and two molecules of dibromine, followed by the formation of a Br-vinyl cation and Br_3^- (Scheme 6). Subsequently, this vinyl bromide cation can either undergo nucleophilic addition of Br^- directly from Br_3^-, to form the dibrominated compounds (**pathway I**) or be stabilized by the Br_3^- counter-anion through a rapid ion-collapse, leading to the formation of intermediates (labelled as **INT1C-*syn*** and **INT1C-*anti*** in Scheme 6) and forming the final product after release of Br_2 (**pathway II**).

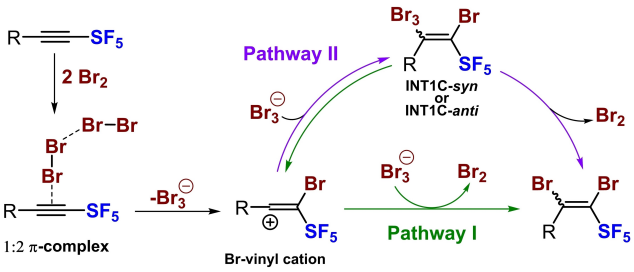

Scheme 6. Proposed mechanisms for dibromination of internal SF_5-alkynes.

To start our computational study, we first investigated the structural characteristics of the cationic intermediates resulting from the electrophilic addition of Br^+ to SF_5-alkyne featuring either an aromatic (R = Ph, as model) or an aliphatic (R = Et, as model) substituent. Our aim was to clarify which structure best described these intermediates: a bridged or an open vinyl-type structure? As depicted in Figure 1, DFT-optimized structures reveal that the C=C double bond interacts in an asymmetric manner with Br^+ for both substituents (Δ(Br–C): 0.7 to 0.9 Å and WBI(C_β–Br): 0.134 to 0.279 *vs* WBI(C_α–Br) ~ 1.0), clearly indicating an open-type structure. A more important dissymmetry appears for the aryl substituent as attested by the bond lengths (Br–C_α ~ 1.875 Å for both alkynes *vs* Br-C_β = 2.766 and 2.600 Å for R = Ph and R = Et, respectively) and the bond angles (Br–C_α–C_β: 121.1 *vs* 109.4°, respectively), consistent with the delocalization of the arene into the vacant $2p^\pi$(C) of the carbocation to stabilize the positive charge. It is important to note

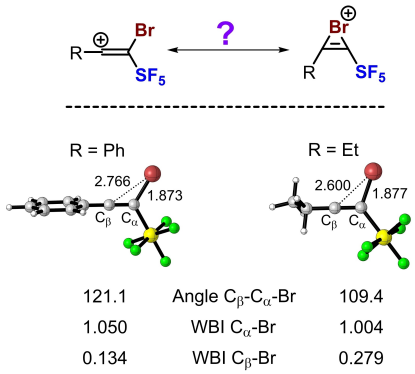

Figure 1. DFT-computed structures of the cationic intermediates after electrophilic addition of Br^+ to SF_5-alkynes featuring an aromatic (Ph) or alkyl (Et) substituent. Distances are given in Å and bond angles in °. All data have been computed at the PCM(DCM)-B3LYP-D3(BJ)/6–311G** level of theory. WBI = Wiberg Bond Index from NBO calculations.

that the dibromination reactions proceeding *via* vinyl cations are typically non-stereospecific,[22c] suggesting that the SF_5 group plays a crucial role in driving the stereospecificity of our reactions. To further support the proposed pathways shown in Scheme 6, we computed the complete reaction profiles for the dibromination reactions involving R–C≡C–SF_5 alkynes with R=Ph (**1b**) or Et (**1v**) (Figure 2a and 2b, respectively). Since the stereochemical determining step cannot be the formation of the vinyl cation, the profiles presented in Figure 2a–b focus directly on how nucleophilic addition occurs over the respective vinyl cations.

When examining the reaction profile involving the aromatic alkyne, our calculations indicate that the ion-pair vinyl-cation/Br_3^- species and the adduct **INT1C-*syn*** can be in equilibrium at RT (activation barrier $\Delta G^{\neq} = 2.3$ kcal/mol *via* **TS1C-*syn*** and $\Delta G_R = -2.3$ kcal/mol in favour of **INT1C-*syn***). In contrary, the formation of **INT1C-*anti*** is clearly less favoured ($\Delta G^{\neq} = 9.9$ kcal/mol *via* **TS1C-*anti*** and $\Delta G_R = +1.2$ kcal/mol). Next, our attempts to locate a transition state corresponding to the release of Br_2 from **INT1C-*syn*** or **INT1C-*anti***, to yield the dibrominated products, failed (**pathway II**). Instead, two transitions states, **TS2C-*syn*** and **TS2C-*anti***, associated to the direct transfer of a bromide atom from the tribromide anion to the vinyl cation were found, leading to the final products **6b"** and **7b"**. These results indicate that the **pathway I** is favoured for the aryl substituent, and that the vinyl cation stabilized by the delocalization of the aromatic substituent, may be sufficiently persistent to enable nucleophilic addition of bromide directly from Br_3^- to produce the final dibrominated products. Notably, the energy difference between the two activation barriers of **TS2C-*syn*** ($\Delta G^{\neq} = 3.6$ kcal/mol) and **TS2C-*anti*** ($\Delta G^{\neq} = 7.6$ kcal/mol) is 4.0 kcal/mol, precisely in line with the experimentally observed stereoselectivity (100:0 **6a"/7a"** in favour of the *syn* addition with R = *p*-Ph-C_6H_4).

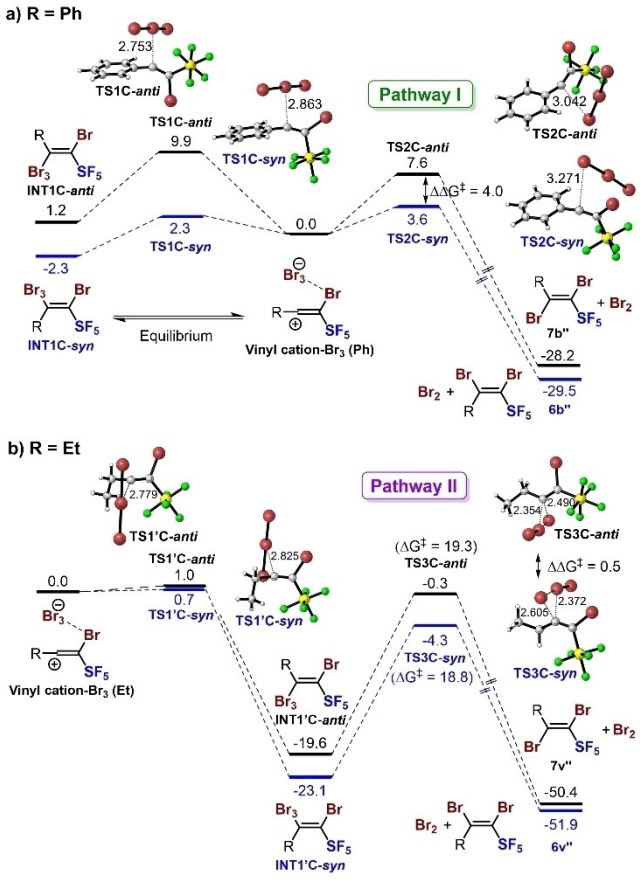

Figure 2. Reaction profiles of the dibromination reactions (conditions C) of SF_5-alkynes featuring: a) an aromatic (R = Ph) or b) an alkyl (R = Et) substituent. Free energy values (ΔG) are given in kcal/mol and main distances in TS in Å. All data have been computed at the PCM(dichloromethane)-B3LYP-D3(BJ)/6–311G** level of theory.

On the other hand, when examining the reaction profile with an alkyl substituent (R = Et), we observed, that both **INT1'C-*syn*** and **INT1'C-*anti*** are promptly generated. As expected, and in contrast to the aromatic substituent, the energy gap between these two intermediates and the initial ion pair is now significant ($\Delta G_R = -23.1$ and -19.6 kcal/mol, respectively) and the ion-collapse transition states (**TS1'C-*syn*** and **TS1'C-*anti***) for the *syn*- and *anti*-additions of the tribromide anion to the vinyl cation, exhibit rather low barriers of less than 1.0 kcal/mol. This implies that these species are not in equilibrium under the reaction conditions, as proposed for the aromatic alkyne, but that the intermediates (**INT1'C**) are the only species in solution. Proceeding from these intermediates, we successfully located the corresponding transition states, **TS3C-*syn*** and **TS3C-*anti***, associated to the release of Br_2 and leading directly to the **6v"** and **7v"** dibrominated products (**Pathway II**). Importantly, the computed activation barriers are 18.8 and 19.3 kcal/mol for **TS3C-*syn*** and **TS3C-*anti***. The slight energy difference ($\Delta\Delta G^{\neq} = 0.5$ kcal/mol) results in a computed stereoselectivity of 70:30 *syn*/*anti*, closely mirroring the experimentally obtained stereoselectivity (78:22 **6t"/7t"** when R = C_8H_{17}).

Next, we also carried out a DFT-study of the hydrohalogenation reaction with SF_5-alkynes in order to clarify the observed differences in stereoselectivity between the two reactions occurring in conditions A or B and to assess the impact of the halogen on the process. We selected the reaction with SF_5-alkyne **1a** as model reaction and focus our attention on the formation of *ß,E* or *ß,Z*-isomers. According to our experimental results, the *ß,E*-isomer was exclusively formed in the presence of a strong acid (hydrogen halide, HX) and the reaction only takes place with an

aromatic substituent. In sharp contrast, *β-Z*-isomer was obtained with a halide salt and the reaction is compatible with both aromatic and alkyl substituents. These facts led us to propose two different mechanisms, according to the experimental conditions (Scheme 7). In conditions A, the initial step of the mechanism involves the protonation of the alkyne, resulting in the formation of a carbocation which can be stabilized by π-donation from the aromatic substituent. Subsequently, a nucleophilic attack by the halide on the carbocation leads to the unique *E*-SF_5-alkenyl halides (Scheme 7, top). On the other hand, when a halide salt (NaX) is involved in the presence of a soft acid AcOH (Conditions B), we propose that the SF_5-alkyne acts as an electrophile, undergoing a nucleophilic attack by the halide. This results in the generation of a carbanion with an increased basicity compared to the initial alkyne. This intermediate is now able to abstract a proton from acetic acid, leading to the predominant or unique *Z*-SF_5-alkenyl halides (Scheme 7, bottom).

According to this mechanistic proposal, we computed the corresponding reaction profiles of the hydrohalogenation processes (halogen = Cl, Br, or I) of alkyne **1a** through pathway A or pathway B. For the latter, we used the reaction with NaX as a model reaction. Additionally, although the hydrofluorination reaction does not occur experimentally through the use of aqueous HF, for the sake of completeness, we also computed the corresponding hydrofluorination reaction of **1a** *via* pathway A. As an illustrative example, both hydroiodination pathways are presented in Figure 3 and the activation barriers for the other halogens are provided in the associated table (for complete reaction profiles see Figures S1–S2). For conditions B, we initially included the Na^+ counter-cation in the calculations in order to consider its potential role over the halide nucleophilic addition. We found that all computed processes are highly exergonic (ΔG_R~−20 kcal/mol), regardless of the halide involved

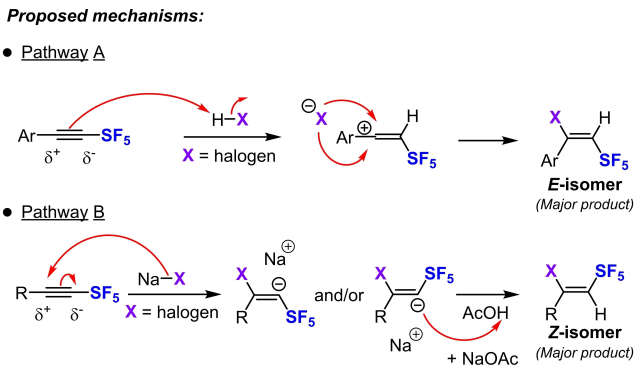

Scheme 7. Mechanistic proposals for the hydrohalogenation of SF_5-alkynes with H–X (pathway A) or Na–X (pathway B); X = halogen.

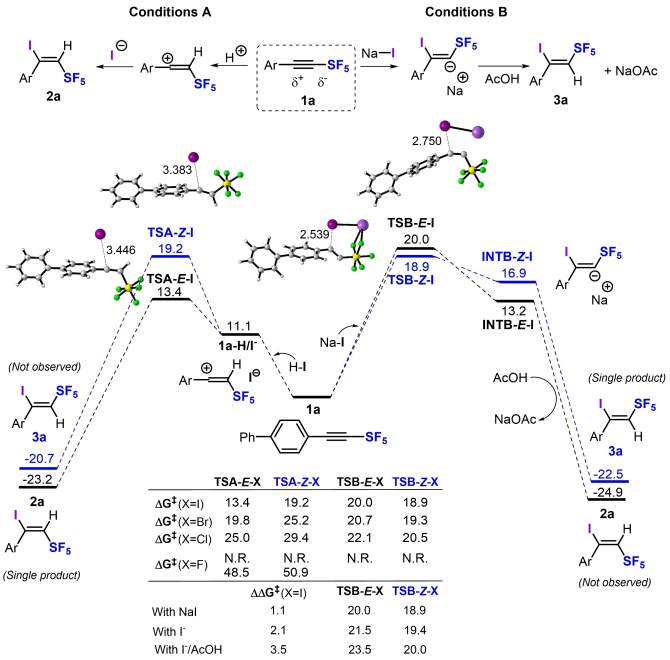

Figure 3. Reaction profiles of the hydroiodination of alkyne **1a** leading to the *E*- or *Z*-isomers through pathway A (left) or pathway B (right, with NaX). For comparison, activation barriers for the hydrohalogenation involving different halides (F, Cl, Br, or I) are given in the table. Free energy values (ΔG) are given in kcal/mol and distances in Å. All data have been computed at the PCM(solvent)-B3LYP-D3(BJ)/6–311G** level of theory. Solvent is toluene for pathway A and acetic acid for pathway B. In the table are also included the data for iodine, in the case of the nucleophilic addition of I^- in absence or presence of AcOH. $\Delta\Delta G^{\ddagger}$, in kcal/mol, corresponds to the energy difference between the activation barriers affording *Z* and *E* isomers.

and that the *E*-isomer is thermodynamically favoured compared to *Z*-isomer ~2.4 kcal/mol. Concerning the activation barriers, clear trends can be identified: (i) all the processes take place with a lower activation barrier when going down in the halogen group from F to I, which is consistent with the nucleophilicity of the halide; (ii) when following pathway A for the same halide, the transition state leading to the *E*-isomer is kinetically favoured over that affording the *Z*-isomer ($\Delta\Delta G^{\ddagger}$ = 2.4 to 5.8 kcal/mol, from F to I); (iii) conversely, when analysing pathway B, the kinetically favoured process corresponds to the formation of the *Z*-isomer ($\Delta\Delta G^{\ddagger}$ = 1.1 to 1.6 kcal/mol, from I to Cl). These results highlight that the stereoselectivity arises from kinetic preferences rather than thermodynamic factors, with formation of the *β-E*-isomer with HX and the *β-Z*-isomer with NaX (X = halogen). Moreover, the activation barriers are accessible under the experimental conditions for I, Br and Cl ($\Delta G^{\ddagger}$ < 25 kcal/mol) and not for F ($\Delta G^{\ddagger}$ ~50 kcal/mol), for which no reaction occurs. By looking more closely at the energy

difference between the 2 activation barriers for the hydroiodination reaction in conditions B ($\Delta\Delta G^{\#} = 1.1$ kcal/mol), we noticed that the gap between the TSs leading to *E*- or *Z*-isomer is not high enough to theoretically confirm the exclusive formation of *Z*-isomer. Considering this, we additionally computed the hydroiodination of alkyne **1a** in absence of the counter-cation to take into account a scenario where Na^+ and I^- are fully dissociated in the polar acetic acid solvent. Our results indicate that the profiles are very similar to the previous ones, with C···I bond lengths in TS and activation barriers of the same order of magnitude. They also indicate that the gap $\Delta\Delta G^{\#}$, in absence of the counter-cation, increases from 1.1 kcal/mol (see table in Figure 3 and Figure S3) to 2.1 kcal/mol, in line with the experimental results. A similar situation was also found when computing the nucleophilic addition of the iodide to **1a** including explicitly one molecule of AcOH. In this case, the *E*:*Z* gap increases even further from 2.1 to 3.5 kcal/mol (see table in Figure 3 and Figure S3).

In order to quantitatively analyse the physical factors responsible for the stereoselectivity, we next applied the Activation Strain Model (ASM) of reactivity.[19] The ASM approach decomposes the electronic energy (ΔE) of a chemical system into two different terms: (i) the strain energy (ΔE_{strain}), representing the energy needed to deform the reactants from their equilibrium geometries during a chemical process and (ii) the interaction energy (ΔE_{int}), which describes both the destabilizing and stabilizing interactions that occur when the increasingly distorted reactants approach each other. We started our ASM study by comparing the two possible nucleophilic attacks (leading to *E*- or *Z*-isomer) of the iodide over the protonated alkyne **1a-H** during pathway A. In order to enable an accurate comparison, we selected two structures along the Intrinsic Reaction Coordinate (IRC) with nearly identical C···I distance of ~3.44 Å close to the TSs (for a plot of the ASM terms along the entire reaction coordinate, see Figure S4). From these results (Table 1, top Path A), we found that the lower electronic energy of the process forming the *E*-isomer ($\Delta E = -39.6$ and -34.8 kcal/mol, for *E*- and *Z*-attack, respectively) is originated by a combination of a lower strain energy (ΔE_{strain}) and a more stabilizing interaction energy (ΔE_{int}) between the reactants ($\Delta E_{strain} = 1.2$ *vs* 4.0 kcal/mol and $\Delta E_{int} = -40.8$ *vs* -38.8 kcal/mol). This lower strain energy can be rationalized by a less distorted structure of the protonated alkyne **1a-H**, as illustrated by the change in the C_{Ar}–C–C angle from 179.9° (equilibrium geometry) to 173.9° or 167.2° for the geometries leading to *E*- or *Z*-isomer (reaction coordinate C···I~3.44 Å). Such bond angle modification leads to a considerable difference in the distortion energy by 2.8 kcal/mol from *E*- to *Z*-attack.

Table 1. Activation Strain Model (ASM) analysis of the hydroiodination of alkyne **1a** with HI (top, pathway A) or NaI (bottom, pathway B) leading to the *E*- or *Z*-isomer, respectively.[24]

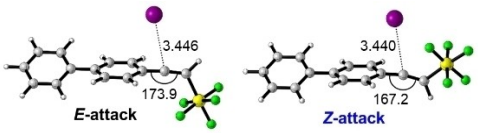

Pathway A	d C···I	ΔE	ΔE_{strain}	ΔE_{int}	Angle C_{Ar}–C–C
E-attack	3.446	−39.6	1.2 (−2.8)	−40.8 (−2.0)	173.9
Z-attack	3.440	−34.8	4.0	−38.8	167.2

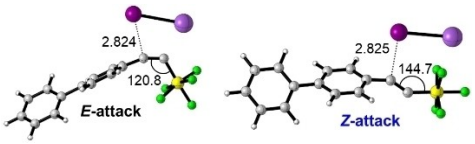

Pathway B	d C···I	ΔE	ΔE_{strain}	ΔE_{int}	Angle C–C–S
E-attack	2.824	8.1	19.6 (−6.7)	−11.5 (+3.7)	120.8
Z-attack	2.825	5.0	12.9	−7.8	144.7

The reaction coordinates have been selected as the C···I distance at ~3.44 Å or ~2.82 Å for pathways A or B. Energy values are given in kcal/mol, distances in Å, and bond angles in °. All data have been computed at the PCM(solvent)-B3LYP-D3(BJ)/6-311G** level of theory. Solvent = toluene or acetic acid for pathway A or B. Into brackets, the variation of ΔE_{strain} and ΔE_{int} using the non-privileged attack as reference point.

In order to understand the *Z*-stereoselectivity under reaction conditions B, we carried out an ASM analysis for the hydroiodination reaction of alkyne **1a** along the reaction coordinate (Figure S5). The ASM results at a quasi-identical C···I distance of 2.82 Å, close to TS, are shown in Table 1, bottom Path B. They revealed that the interaction energy is again more stabilizing for the *E*-attack (−11.5 kcal/mol) compared to the *Z*-attack (−7.8 kcal/mol). However, this difference is lower than that found in the distortion energy (ΔE_{strain} = 19.6 *vs* 12.9 kcal/mol for the *E*- *vs* *Z*-attack). Therefore, the experimentally observed *Z*-stereoselectivity under reaction conditions B finds its origin uniquely by a lower strain energy. As previously, this strain energy difference can be readily understood from a more distorted geometry of the alkyne **1a** in the *E*-attack. Indeed, the angle C–C–S varies from 180.0° in the equilibrium geometry of **1a** to 120.8° or 144.7° in the selected geometries at the reaction coordinate C···I of 2.82 Å for the *E*- or *Z*-attack, respectively. As the interaction energy plays also a significant role for understanding the *E*-stereoselectivity observed during the hydroiodination process under reaction conditions A, we next applied the Energy Decomposition Analysis (EDA) method to quantitatively analyse this interaction. The EDA approach decomposes the ΔE_{int} term into different and chemically meaningful terms, namely, the electrostatic interaction (ΔV_{elstat}), the orbital interaction (ΔE_{orb}), the Pauli repulsion (ΔE_{Pauli}) and the dispersion energy (ΔE_{disp}). Solvation effects (ΔE_{solv}) were also quantified by means of the Conductor like Screening Model (COSMO).[19] The terms deriving from our EDA analysis are shown in Table 2. The orbital interaction ΔE_{orb}, the solvation ΔE_{solv} and the dispersion ΔE_{disp} energies are more stabilizing for the *Z*-attack ($\Delta\Delta E_{orb}$ = 5.2; $\Delta\Delta E_{disp}$ = 1.0; $\Delta\Delta E_{solv}$ = 1.1 kcal/mol) than for the *E*-attack, suggesting that these factors are not responsible at all for the experimentally observed *E*-stereoselectivity.

On the contrary, the Pauli repulsion ΔE_{Pauli}, which quantify steric repulsion, is considerably lower for the process affording the *E*-isomer ($\Delta\Delta E_{Pauli}$ = −6.5 kcal/mol). This factor and to a lesser extent the electrostatic interaction ($\Delta\Delta V_{elest}$ = −2.3 kcal/mol) are therefore responsible for the *E*-selectivity. In order to find the reason of the lower Pauli repulsion for the *E*-attack in conditions A, we conducted a Kohn-Sham molecular orbital analysis. To this end, we selected the same structures we used during the ASM/EDA studies, at the consistent distance of C···I of ~3.44 Å, and we analyzed the overlap (S) between occupied orbitals, which is the sole factor affecting the ΔE_{Pauli} term. Among all the plausible occupied-occupied orbital interactions between the iodide and the protonated alkyne (**1a-H**), we searched those where the orbital overlap differs considerably between the *E*- or *Z*-attack. As illustrated in Figure 4, we found that the interactions between the well-oriented lone pair of the iodide and the HOMO or HOMO-4 (π system involving $2p^{\pi}(C_{\beta})$ and the aromatic system) of the **1a-H** are much larger and therefore much more destabilizing for the attack leading to the *Z*-isomer compared to the attack leading to the *E*-isomer (S*100(HOMO-HOMO) = 2.54 *vs* 1.52 and S*100(HOMO-HOMO-4) = 5.48 *vs* 1.56). We also found an important difference in overlap between the same iodide lone pair and the HOMO-11 of **1a-H**, which corresponds mainly to a combination of the lone pairs associated with the fluorine atoms of the SF_5 group (Figure S6). As expected, this overlap is negligible for the *E*-attack (S*100 = 0.04) but extremely relevant for the *Z*-attack

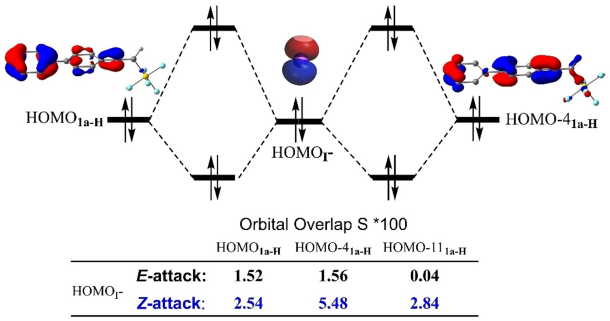

Figure 4. Schematic representation of the interaction between occupied molecular orbitals of the iodide and the protonated alkyne **1a-H** involved in the Pauli repulsion term. Orbital overlaps multiplied by 100 (S*100) are given for the attack leading to the *E*- or *Z*-isomers. Plot of the HOMO and HOMO-4 (cutoff : 0.05) of the protonated alkyne **1a-H** and the HOMO of I^- in geometries close to TSs at C···I of ~3.44 Å. Hydrogen atoms have been omitted for clarity.

Table 2. Energy Decomposition Analysis (EDA) of the stereodivergent hydroiodination of alkyne **1a** under reaction conditions A.

Pathway A	d C···I	ΔE_{int}	ΔE_{Pauli}	ΔV_{elstat}	ΔE_{Orb}	ΔE_{Disp}	ΔE_{solv}
E-attack	3.446	−39.5	26.6	−86.6 (72.1%)	−28.1 (23.4%)	−5.4 (4.5%)	54.0
Z-attack	3.440	−38.0	33.1	−84.3 (68.0%)	−33.3 (26.9%)	−6.4 (5.2%)	52.9

The reaction coordinates have been selected as the C···I distance of ~3.44 Å. Energy values are given in kcal/mol. Data computed at COSMO(Toluene)-ZORA-B3LYP-D3(BJ)/QZ4P//PCM(Toluene)-B3LYP-D3(BJ)/6-311G** level of theory. Contribution (in %) of each stabilizing term in relation to the sum of all stabilizing terms, are given into brackets.

(S*100 = 2.84). To emphasize the primary details, the combination of ASM, EDA and Orbital analyses evidences that the stereoselectivity originates from a less important deformation (ΔE_{strain}) of the reactants during the hydroiodination processes. In addition, the formation of the *E*-isomer in conditions A is also driven by steric effects, as confirmed by a lower overlap between the lone pair of I- and the π-occupied molecular orbitals of the protonated alkyne involving $2p^{\pi}(C_{\beta})$ and the aromatic system or F lone pairs of SF_5, which reduce the repulsive occupied-occupied orbital interactions.

Finally, several functionalizations of iodoolefins **2a** and **3a** were carried out (Scheme 8). First, we performed an evaluation of the compatibility of **2a** and **3a** with different bases. Indeed, iodo-olefins are likely to undergo dehydrohalogenation under basic conditions to give back SF_5-alkyne **1a** (See Table S1 for details). We first identified that *E*-iodo-olefin **2a** is much more sensitive to base than **3a**, leading to decomposition with most of the bases tested. In contrast, *Z*-iodo-olefin **3a** is much more robust and compatible with Et_3N or Hünig's base for instance. We then evaluated various post-functionalizations with both compounds **2a** and **3a** but those transformations are out of the scope of the present study and were not fully optimized. As evaluated earlier, **2a** was prone to decomposition, so we focused efforts on the *Z*-iodo-olefin **3a**.

We developed for the very first time effective palladium-catalyzed cross-coupling reactions, which allow the introduction of an alkyl (**8a**), a vinyl (**9a**), an aryl (**10a**), an alkynyl (**11a**) or even a cyano group (**12a**). With diethylzinc, a 57:43 ratio of coupling product **8a** and reduced product **5a** (resulting of *β*-hydride elimination) was obtained, but they can be separated and isolated in 45 and 35% yield, respectively. Reduction of either *E*- and *Z*-iodoolefins **2a** and **3a** with tris(trimethylsilyl)silane was performed with a catalytic amount of triethylborane, leading to high yields of the unique *Z*-reduced product **13a**. This can easily be explained by the formation of the most stable radical intermediate.[6b] The *E*-isomer **5a** could be obtained in 71% yield by performing a palladium-catalyzed hydrodeiodination with triethylsilane.

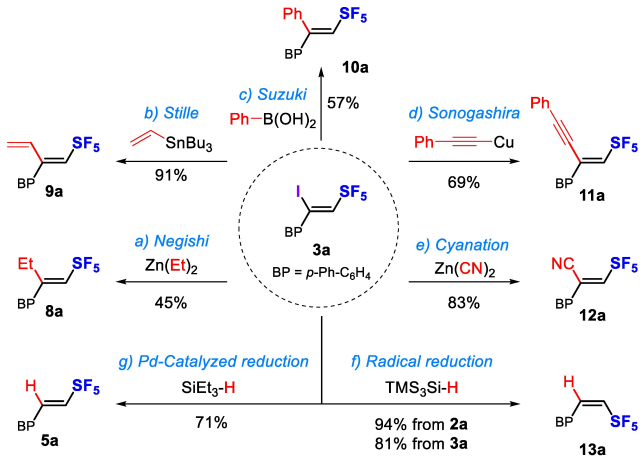

a) Pd(P*t*-Bu$_3$)$_2$ 10 mol%, ZnEt$_2$ (1.2 equiv.), THF, - 20 °C, 4h; b) PdCl$_2$(amphos)$_2$ (5 mol%), tributyl(vinyl)stannane (1.05 equiv), Et$_3$N (1 equiv.), THF, 80 °C, 16h; c) Pd(OAc)$_2$ (20 mol%), XPhos (40 mol%), K$_2$CO$_3$ (2 equiv.), PhB(OH)$_2$ (1.5 equiv.), toluene:H$_2$O 10:1, 110 °C, 15h; d) Pd(PPh$_3$)$_4$ (20 mol%), (phenylethynyl)copper (1.5 equiv.), THF, 80 °C, 15h; e) CuI (1.2 equiv.), Zn(CN)$_2$ (1.0 equiv.), DMF, 100 °C, 72h; f) TMSSiH (1.5 equiv.), BEt$_3$ (10 mol%), CH$_2$Cl$_2$, r.t., 2h; g) Pd(PPh$_3$)$_4$ (10 mol%), Et$_3$SiH (2 equiv.), THF, 80 °C, 16h.

Scheme 8. Post-funtionalizations of *β*-iodo SF_5-olefins.

Conclusion

In summary, we have validated the hypothesis that SF_5-alkynes can react both as electrophile and nucleophile by developing regioselective and stereodivergent methodologies to perform independently *β*,*Z*- and *β*,*E*-selective hydroiodination of SF_5-alkynes with excellent selectivities. The transformation can be extended easily to bromination and chlorination, while fluorination required some adjustments. Dihalogenation with I_2, Br_2 and ICl yielded in all cases the *cis*-dihalogenated isomers as major products alongside with full regioselectivity for ICl. DFT calculations have provided a detailed description of the mechanisms for the dihalogenation and the hydrohalogenation reaction of SF_5-alkynes using strong or soft acidic conditions in the presence of halide sources. We rationalized the privileged *cis*-stereochemistry of the dibromination reaction of SF_5-alkynes depending on the alkyne substituents. We found that the aromatic substituent stabilizes the Br-vinyl cation formed after electrophilic addition of Br^+ on the alkyne, allowing the direct transfer of bromide from the Br_3^- anion with complete *cis*-selectivity. On the contrary, with alkyl substituent, the vinyl cation is considerably less stable and a rapid ion-collapse occurs with the Br_3^- anion. Then, the release of Br_2 leads to the final dibrominated products as mixture of *syn*/*anti* addition products. Concerning hydrohalogenation reactions of SF_5-alkynes using strong or soft acidic conditions in the presence of halide sources, two mechanistic scenarios occur. With strong acids, the reaction proceeds *via* protonation of the SF_5-alkyne followed by a nucleophilic attack of the halide. Conversely, with the aid of soft acid, the halide nucleophilic attack on the alkyne occurs first with a subsequent protonation of the corresponding anionic intermediate. We extensively analyzed the *E*- and *Z*-stereodivergence of these processes using the ASM method. We found that *E*-stereoselectivity is a result of the combination of a lower strain energy and a stronger stabilizing interaction between the reactants, while the *Z*-stereoselectivity is due solely to the lower energy requirement to distort the reactants. With the help of

the EDA method, we highlighted that the stronger interaction between the reactants upon the formation of *E*-alkenyl halides is due to a smaller overlap between the main occupied orbitals of the reactants, ultimately leading to lower Pauli repulsion. Several post-functionalization reactions of these halo-olefins were developed which clearly highlight the great synthetic potential of these building blocks.

Experimental Section

Conditions A1–A3: General Procedure for the *ß-E* Hydrohalogenation of SF_5-alkynes using Halides in TFA

In a flask, the SF_5-alkyne **1** (1 equiv.) was mixed with TFA (10 mL/mmol). Then, the halide (For iodide: NaI or TBAI; for bromide: nBu$_4$PBr; for chloride: Me$_4$NCl (1.5 equiv.)) was added. The mixture was stirred at 70 °C for 1 h until completion of the reaction as followed by ^{19}F-NMR or TLC. The mixture was washed with water and extracted with 3 volumes of dichloromethane. The organic layers were combined, dried with $MgSO_4$, filtered, concentrated under vacuum and purified over silica gel column chromatography affording the *ß-E*-iodo SF_5-olefin **2**.

Conditions B1–B3: General Procedure for the *ß-Z* hydrohalogenation of SF_5-alkynes using Halides in AcOH

In a flask, the SF_5-alkyne **1** (1 equiv.) was dissolved in AcOH (10 mL/mmol). Then, the halide (for iodide: NaI or TBAI; for bromide: nBu$_4$PBr; for chloride: Me$_4$NCl (1.5 equiv.)) was added. The solution was stirred at 110 °C for 15 h. The completion of the reaction was followed by ^{19}F-NMR or TLC. The mixture was washed with water and extracted with 3 volumes of dichloromethane. The organic layers were combined, dried with $MgSO_4$, filtered, concentrated under vacuum and purified over silica gel column chromatography affording the *ß-Z*-iodo SF_5-olefin **3**.

Conditions C: General Procedure for the Dihalogenation of SF_5-alkynes

In a flask, the SF_5-alkyne **1** (1 equiv.) was dissolved in dichloromethane. Then the dihalogen (either I_2, ICl or Br_2, 1–2 equiv.) was added, the reaction was stirred at room temperature for 2 h and followed by ^{19}F-NMR or TLC. The mixture was concentrated under vacuum and the crude purified over silica gel column chromatography to give *Z*-(dialogeno)vinyl-SF_5 **6** as major product.

The CCDC numbers - [CCDC 2303456, **2aa**], [CCDC 2303459, **2ab**], [CCDC 2303460, **3ab**], [CCDC 2303462, **2ac**], [CCDC 2251406, **2k**], and [CCDC 2303461, **3a**] – contains the supplementary crystallographic data for this paper. These data can be obtained free of charge from The Cambridge Crystallographic Data Centre *via* www.ccdc.cam.ac.uk/structures.

Acknowledgements

This work is supported by the ANR SULFIVE project (grant ANR-PRC-21-CE07-0042) of the French National Research Agency (ANR), Université de Haute-Alsace, Université de Strasbourg, Normandie Université, and CNRS. The authors acknowledge Didier Le Nouën (LIMA UMR7042 CNRS-Unistra-UHA), Corinne Bailly and Nathalie Gruber (Service de radiocristallographie de la Fédération de Chimie Le Bel FR 2010) who contributed, by their valuable technical and scientific support in NMR and X-ray diffraction, to the achievement of this research project. The "Direction du Numérique" of the Université de Pau et des Pays de l'Adour and Mésocentre de Calcul Intensif Aquitain (MCIA) are acknowledged for computational facilities. This work was also performed using HPC resources from GENCI-IDRIS (Grant 2022–2023-[project AD010800045R1-R2]).

References

[1] For general reviews about SF_5, see: a) R. Kordnezhadian, B.-Y. Li, A. Zogu, J. Demaerel, W. M. De Borggraeve, E. Ismalaj, *Chem. Eur. J.* **2022**, *28*, e202201491; b) M. Magre, S. Ni, J. Cornella, *Angew. Chem. Int. Ed.* **2022**, *61*, e202200904 ; c) G. Haufe, *Tetrahedron* **2022**, *109*, 132656; d) D. Rombach, H.-A. Wagenknecht, *Synthesis* **2022**, *54*, 4883; e) Y. Kraemer, E. N. Bergman, A. Togni, C. R. Pitts, *Angew. Chem. Int. Ed.* **2022**, *61*, e202205088 ; f) D. J. Burton, Y. Wang, V. Bizet, D. Cahard, in *Encyclopedia of Reagents for Organic Synthesis*, **2020**, P1–7; g) Ponomarenko, G.-V. Röschenthaler, in *Frontiers of Organofluorine Chemistry*, **2019**, pp. 251–279; h) P. R. Savoie, J. T. Welch, *Chem. Rev.* **2015**, *115*, 1130.

[2] a) M. Sani, M. Zanda, *Synthesis* **2022**, *54*, 4184; b) V. Debrauwer, I. Leito, M. Lõkov, S. Tshepelevitsh, M. Parmentier, N. Blanchard, V. Bizet, *ACS Org. Inorg. Au* **2021**, *1*, 43; c) P. Beier, in *Emerging Fluorinated Motifs: Synthesis, Properties and Applications*; D. Cahard, J.-A.Ma, Eds.: Wiley-VCH: Weinheim, Germany, **2020**; *Vol 2*, pp 551–570; d) B. Cui, N. Shibata, *Phosphorus Sulfur Silicon Relat. Elem.* **2019**, *194*, 658; e) P. Das, E. Tokunaga, N. Shibata *Tetrahedron Lett.* **2017**, *58*, 4803; f) O. S. Kanishchev, W. R. Dolbier, in *Advances in Heterocyclic Chemistry*, E. F. V. Scriven, C. A. Ramsden, Eds.; Academic Press, **2016**; *Vol. 120*, pp 1–42.

[3] a) M. Inoue, Y. Sumii, N. Shibata, *ACS Omega* **2020**, *5*, 10633; b) L. Xing, T. Honda, L. Fitz, I. Ojima, in *Fluorine in Life Sciences: Pharmaceuticals, Medicinal Diagnostics, and Agrochemicals* (Eds.: G. Haufe, F. R. Leroux), Academic Press, 2019, pp. 181–211; c) M. F. Sowaileh, R. A. Hazlitt, D. A. Colby, *ChemMedChem* **2017**, *12*, 1481.

[4] a) R. Gujjar, F. El Mazouni, K. L. White, J. White, S. Creason, D. M. Shackleford, X. Deng, W. N. Charman, I. Bathurst, J. Burrows, D. M. Floyd, D. Matthews, F. S. Buckner, S. A. Charman, M. A. Phillips, P. K. Rathod, *J. Med. Chem.* **2011**, *54*, 3935; b) J. T. Welch, D. S. Lim,

Bioorg. Med. Chem. **2007**, *15*, 6659; c) D. S. Lim, J. S. Choi, C. S. Pak, J. T. Welch, *J. Pestic. Sci.* **2007**, *32*, 255.
[5] J. M. W. Chan, *J. Mater. Chem. C* **2019**, *7*, 12822.
[6] Selected examples: a) Y. Kraemer, J. Buldt, A. Stephens, W.-Y. Kong, A. Ragan, Z. Haidar, A. Patel, J. Fettinger, D. Tantillo, C. R. Pitts, *ChemRxiv.* **2023**, DOI: 10.26434/chemrxiv-2023-dwkhg. This content is a preprint and has not been peer-reviewed b) M. Birepinte, P. A. Champagne, J.-F. Paquin, *Angew. Chem. Int. Ed.* **2022**, *61*, e202112575; c) J.-Y. Shou, F.-L. Qing, *Angew. Chem. Int. Ed.* **2022**, *61*, e202208860; d) J.-Y. Shou, X.-H. Xu, F.-L. Qing, *J. Fluorine Chem.* **2022**, *261–262*, 110018; e) Y. Kraemer, C. Ghiazza, A. N. Ragan, S. Ni, S. Lutz, E. K. Neumann, J. C. Fettinger, N. Nöthling, R. Goddard, J. Cornella, C. R. Pitts, *Angew. Chem. Int. Ed.* **2022**, *61*, e202211892; f) D. Rombach, B. Birenheide, H.-A. Wagenknecht, *Chem. Eur. J.* **2021**, *27*, 8088; g) A. Gilbert, P. Langowski, M. Delgado, L. Chabaud, M. Pucheault, J.-F. Paquin, *Beilstein J. Org. Chem.* **2020**, *16*, 3069; h) A. Gilbert, J.-F. Paquin, *J. Fluorine Chem.* **2019**, *221*, 70.
[7] For recent examples, see: a) R. Kordnezhadian, T. De Bels, K. Su, L. Van Meervelt, E. Ismalaj, J. Demaerel, W. M. De Borggraeve, *Org. Lett.* **2023**, *25*, 8947; b) T. Gatzenmeier, Y. Liu, M. Akamatsu, T. Okazoe, K. Nozaki, *ChemRxiv.* **2023**, DOI: 10.26434/chemrxiv-2023-jzn11. This content is a preprint and has not been peer-reviewed c) R. Kordnezhadian, A. Zogu, C. Borgarelli, R. Van Lommel, J. Demaerel, W. M. De Borggraeve, E. Ismalaj, *Chem. Eur. J.* **2023**, *29*, e202300361; d) K. Tanagawa, Z. Zhao, N. Saito, N. Shibata, *Bull. Chem. Soc. Jpn.* **2021**, *94*, 1682; e) C. R. Pitts, D. Bornemann, P. Liebing, N. Santschi, A. Togni, *Angew. Chem. Int. Ed.* **2019**, *58*, 1950; f) J. Ajenjo, B. Klepetářová, M. Greenhall, D. Bím, M. Culka, L. Rulíšek, P. Beier, *Chem. Eur. J.* **2019**, *25*, 11375; g) P. Das, E. Tokunaga, N. Shibata, *Tetrahedron Lett.* **2017**, *58*, 4803; h) B. Cui, M. Kosobokov, K. Matsuzaki, E. Tokunaga, N. Shibata, *Chem. Commun.* **2017**, *53*, 5997; i) B. Cui, S. Jia, E. Tokunaga, N. Saito, N. Shibata, *Chem. Commun.* **2017**, *53*, 12738; j) P. Das, E. Tokunaga, N. Shibata, *Tetrahedron Lett.* **2017**, *58*, 4803.
[8] L. Popek, T. M. Nguyen, N. Blanchard, D. Cahard, V. Bizet, *Tetrahedron* **2022**, *117–118*, 132814.
[9] a) K. Iwaki, K. Maruno, O. Nagata, N. Shibata, *J. Org. Chem.* **2022**, *87*, 6302; b) K. Iwaki, K. Tanagawa, S. Mori, K. Maruno, Y. Sumii, O. Nagata, N. Shibata, *Org. Lett.* **2022**, *24*, 3347; c) K. Maruno, K. Niina, O. Nagata, N. Shibata, *Org. Lett.* **2022**, *24*, 1722; d) K. Maruno, K. Hada, Y. Sumii, O. Nagata, N. Shibata, *Org. Lett.* **2022**, *24*, 3755; e) P. Das, K. Niina, T. Hiromura, E. Tokunaga, N. Saito, N. Shibata, *Chem. Sci.* **2018**, *9*, 4931.
[10] For recent examples of hydroelementation of SF_4X and SF_5-alkynes, see: a) L. Popek, J. J. Cabrera-Trujillo, V. Debrauwer, N. Blanchard, K. Miqueu, V. Bizet, *Angew. Chem. Int. Ed.* **2023**, *62*, e202300685; b) T. Aggarwal, K. Hada, Y. Murata, Y. Sumii, K. Tanagawa, K. Niina, S. Mori, J. Escorihuela, N. Shibata, *Angew. Chem. Int. Ed.* **2023**, *62*, e202307090; c) J. O. Wenzel, F. Jester, A. Togni, D. Rombach, *Chem. Eur. J.* **2023**, *30*, e202304015; d) H. Kucher, J. O. Wenzel, D. Rombach, *ChemRxiv.* **2022**, DOI 10.26434/chemrxiv-2022-01jhn. This content is a preprint and has not been peer-reviewed.
[11] For examples of iodination of CF_3-alkynes, see: a) F.-L. Qing, W.-Z. Gao, J. Ying, *J. Org. Chem.* **2000**, *65*, 2003; b) T. Yamazaki, T. Yamamoto, R. Ichihara, *J. Org. Chem.* **2006**, *71*, 6251; c) T. Konno, J. Chae, T. Tanaka, T. Ishihara, H. Yamanaka, *J. Fluorine Chem.* **2006**, *127*, 36; d) X.-G. Zhang, M.-W. Chen, P. Zhong, M.-L. Hu, *J. Fluorine Chem.* **2008**, *129*, 335.
[12] a) S. Aït-Mohand, W. R. Dolbier, *Org. Lett.* **2002**, *4*, 3013; b) T. M. Nguyen, L. Popek, D. Matchavariani, N. Blanchard, V. Bizet, D. Cahard, *Org. Lett.* **2024**, *26*, 365–369; c) W. R. Dolbier, S. Aït-Mohand, T. D. Schertz, T. A. Sergeeva, J. A. Cradlebaugh, A. Mitani, G. L. Gard, R. W. Winter, J. S. Thrasher, *J. Fluorine Chem.* **2006**, *127*, 1302.
[13] R. Gauthier, M. Mamone, J.-F. Paquin, *Org. Lett.* **2019**, *21*, 9024.
[14] T. M. Nguyen, C. Y. Legault, N. Blanchard, V. Bizet, D. Cahard, *Chem. Eur. J.* **2023**, *29*, e202302914.
[15] For analogous reaction with CF_3-alkynes, see: a) G. Prié, M. Abarbri, J. Thibonnet, J.-L. Parrain, A. Duchêne, *New J. Chem.* **2003**, *27*, 432; b) P.-A. Wang, M.-Z. Deng, R.-Q. Pan, S.-Y. Zhang, *J. Fluorine Chem.* **2003**, *124*, 93; c) G. Prié, J. Thibonnet, M. Abarbri, A. Duchêne, J.-L. Parrain, *Synlett* **1998**, 839.
[16] X-ray diffraction presented using CYLview20; Legault, C. Y., Université de Sherbrooke, **2020** (http://www.cylview.org).
[17] For examples of dihalogenation of CF_3-alkynes, see: a) B. J. Murray, T. G. F. Marsh, D. S. Yufit, M. A. Fox, A. Harsanyi, L. T. Boulton, G. Sandford, *Eur. J. Org. Chem.* **2020**, *2020*, 6236; b) M. N. Bobrovnikov, *Russ. J. Org. Chem.* **1994**, *30*, 1767.
[18] Unless otherwise noted, the stability of all the halogenated products is excellent. We observed that diiodination reaction needs light to proceed but at the same time **6a**, **6i** seems to be light sensitive. Reactions with ICl and Br_2 works the same way under day light or in the dark.
[19] See supporting information for more experimental and computational details.
[20] Y. Murata, K. Hada, T. Aggarwal, J. Escorihuela, N. Shibata, *Angew. Chem. Int. Ed.* **2024**, *63*, e202318086.
[21] R. Guo, X. Qi, H. Xiang, P. Geaneotes, R. Wang, P. Liu, Y.-M. Wang, *Angew. Chem. Int. Ed.* **2020**, *59*, 16651.
[22] a) T. Okazaki, K. K. Laali, *J. Org. Chem.* **2005**, *70*, 9139; b) M. Smith, J. March, *March's Advanced Organic Chemistry Reactions, Mechanisms, and Structure* (*6th ed.*). Wiley Interscience: New York. 2007; c) F. A. Carey, R. J. Sundberg, *Advanced Organic Chemistry, Part A Structure and Mechanisms* (*5th ed.*). New York Springer. 2007.
[23] a) R. Bianchini, C. Chiappe, G. Lo Moro, D. Lenoir, P. Lemmen, N. Goldberg, *Chem. Eur. J.* **1999**, *5*, 1570;

b) G. Bellucci, R. Bianchini, R. Ambrosetti, *J. Am. Chem. Soc.* **1985**, *107*, 2464; c) H. Slebocka-Tilk, R. G. Ball, R. S. Brown, *J. Am. Chem. Soc.* **1985**, *107*, 4504; d) R. Bianchini, C. Chiappe, R. Herges, J. Grunenberg, D. Lenoir, P. Lemmen, *Angew. Chem.* **1997**, *109*, 1340; *Angew. Chem. Int. Ed.* **1997**, *36*, 1284.

[24] It is noteworthy that for conditions B, the ASM analysis has also been carried out for I^- alone (without the presence of the counter-cation) and compared to the results with NaI. The conclusions are identical (see comparative table in SI, table S2).

RESEARCH ARTICLE

Ambiphilic Reactivity of SF_5-Alkynes Applied to Regioselective and Stereodivergent Halogenation Reactions: An Experimental and Theoretical Case Study

Adv. Synth. Catal. **2024**, *366*, 1–14

D. Matchavariani, L. Popek, J. J. Cabrera-Trujillo, T. M. Nguyen, N. Blanchard, K. Miqueu*, D. Cahard*, V. Bizet*